

Feasibility and Reproducibility of Neurochemical Profile Quantification in the Human Hippocampus at 3T

Petr Bednařík^{1,2,3}, Amir Moheet², Dinesh K. Deelchand¹, Uzay E. Emir^{1,*}, Lynn E. Eberly⁴, Martin Bareš^{5,6}, Elizabeth R. Seaquist², and Gülin Öz¹

¹ Center for Magnetic Resonance Research, Department of Radiology, Medical School, University of Minnesota, Minneapolis, MN, United States

² Division of Endocrinology and Diabetes, Department of Medicine, University of Minnesota, Minneapolis, MN, United States

³ Multimodal and Functional Neuroimaging Research Group, Central European Institute of Technology, CEITEC MU, Brno, Czech Republic

* *Present address:* Oxford Centre for Functional MRI of the Brain (FMRIB), John Radcliffe Hospital, University of Oxford, Headington, Oxford OX3 9DU, UK

⁴ Division of Biostatistics, School of Public Health, University of Minnesota, Minneapolis, MN, United States

⁵ Behavioral and Social Neuroscience Research Group, Central European Institute of Technology, CEITEC MU, Brno, Czech Republic

⁶ First Department of Neurology, Masaryk University and St. Anne's Teaching Hospital, Brno, Czech Republic

Corresponding author:

Petr Bednařík, M.D.
Center for Magnetic Resonance Research
University of Minnesota
2021 Sixth Street SE
Minneapolis, MN 55455, USA

Office Phone: +1 612-626-2001
Fax: +1 612-626-2004
Email: bedna028@umn.edu

Word count: 5842 (main text + bibliography + figure captions)

Abstract summary:

Hippocampal dysfunction is known to be associated with several neurological and neuropsychiatric disorders such as Alzheimer's disease, epilepsy, schizophrenia and depression, therefore there has been significant clinical interest to study hippocampal neurochemistry. However the hippocampus is a challenging region to study using ^1H MRS, hence the use of MRS for clinical research in this region has been limited. Therefore, our goal was to investigate the feasibility of obtaining high quality hippocampal spectra that allow reliable quantification of a neurochemical profile and to establish inter-session reproducibility of hippocampal MRS, including reproducibility of voxel placement, spectral quality and neurochemical concentrations. Ten healthy volunteers were scanned in two consequent sessions using a standard clinical 3T MR scanner. Neurochemical profiles were obtained with a short-echo ($\text{TE}=28\text{ms}$) semi-LASER localization sequence from a relatively small ($\sim 4\text{mL}$) voxel that covered $\sim 62\%$ of the hippocampal volume as calculated from segmentation of T_1 -weighted images. Voxel composition was highly reproducible between sessions, with test-retest coefficients-of-variance (CV) of 3.5% and 7.5% for gray and white matter volume fraction, respectively. Excellent signal-to-noise ratio (53.6 ± 7.6 based on the *N*-acetylaspartate (NAA)-methyl peak in non-apodized spectra) and linewidths (8.7 ± 0.8 Hz for water) were achieved reproducibly in 10 subjects. The spectral quality allowed quantification of NAA, total choline, total creatine, *myo*-inositol and glutamate with high scan-rescan reproducibility ($\text{CV} \leq 6\%$) and quantification precision (Cramér-Rao lower bounds, $\text{CRLB} < 9\%$). Seven other metabolites, including glucose, glutathione and ascorbate, were quantified with CRLB and scan-rescan CV below 30%. Therefore, the highly optimized, short echo semi-LASER sequence together with FASTMAP shimming substantially improved the reproducibility and number of quantifiable metabolites relative to prior reports. In addition, the between-session variation in metabolite concentrations, as well as CRLB were lower than between-subject variation of the concentrations for most metabolites indicating that the method has the sensitivity to detect inter-individual differences in the healthy brain.

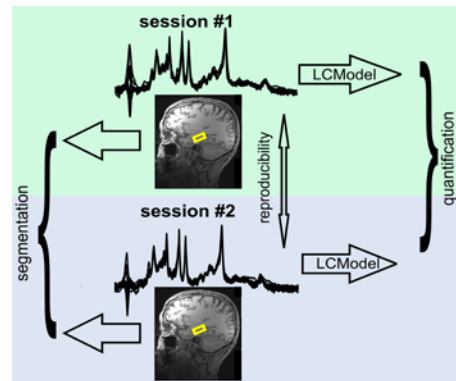
Keywords: MRS, human hippocampus, 3T, reproducibility, quantification precision, coefficient of variation, segmentation, metabolites

Graphical abstract:

Feasibility and Reproducibility of Neurochemical Profile Quantification in the Human Hippocampus at 3T

P. Bednařík, A. Moheet, D.K. Deelchand, U.E. Emir, L.E. Eberly, M.Bareš, E.R. Seaquist, and G. Öz

The feasibility of obtaining and quantifying high-quality proton MR spectra acquired from a small hippocampal voxel (~4mL) was investigated in this study with a test-retest design in 10 healthy subjects. The study was conducted using standard clinical hardware (3T Siemens scanner) benefiting from full-signal intensity semi-LASER localization sequence. The potential utility for clinical research was considered by evaluating the variance in metabolite concentrations along with the consistency in the voxel positioning assessed by segmentation of anatomical images.



Abbreviations used:

Asc

ascorbate

Asc+GSH

ascorbate+guthathione

Asp

aspartate

Cr

Creatine

CRLB

Cramer–Rao lower bound

CSD

chemical shift displacement

CSF

cerebrospinal fluid

CV

coefficient of variation

FID

free induction decay

GABA

γ -aminobutyric acid

Glc

glucose

Glc+Tau

glucose+taurine

Gln

glutamine

Glu

glutamate

Glx

glutamate+glutamine

GM

gray matter

GPC

glycerophosphocholine

LCModel

	linear combination model
LW	linewidth
MPRAGE	magnetization prepared rapid gradient echo
Myo-Ins	myo-inositol
NAA	N-acetylaspartate
NAAG	N-acetylaspartylglutamate
OVS	outer-volume suppression
PCho	phosphocholine
PCr	phosphocreatine
PE	phosphorylethanolamine
SD	standard deviation
scyllo-Ins	scyllo-inositol
SNR	signal-to-noise ratio
Tau	taurine
tCho	total choline
tCr	total creatine
tNAA	total N-acetylaspartate
VOI	volume of interest
WM	white matter.

INTRODUCTION:

The hippocampus, a brain structure located deep in the temporal lobe, plays an essential role in learning, memory formation (1) and stress regulation (2). Hippocampus dysfunction is thought to be involved in several neurological, psychiatric and metabolic diseases, including Alzheimer's disease (3), temporal lobe epilepsy (4), schizophrenia (5), and diabetes (8). Importantly, hippocampal function can be affected both by pharmacological and non-pharmacological treatments, such as exercise training (9,10).

Therefore there is great interest in studying the hippocampus using proton magnetic resonance spectroscopy (^1H MRS) to elucidate disease-related neurochemical alterations and their reversal with therapies. As a complementary modality to conventional structural MRI, MRS can be used to investigate changes in cell density, cell type or biochemical composition of neural tissue. Thereby spectroscopy can differentiate pathologies indistinguishable by structural MRI (11) and is sensitive to early cellular changes in central nervous system (CNS) diseases. For instance, MRS may help guide critical presurgical decisions in pharmacologically intractable epilepsy (12), and provide surrogate markers to monitor disease progression or treatment effects in trials (14). Despite this potential, the role of hippocampal spectroscopy has been limited in clinical research due to challenges associated with obtaining consistently high quality MRS data from this region.

Prior ^1H MRS studies reported hippocampal concentrations of 3-5 neurochemicals only (3,15), even at 3T with the short echo approach (16). Several reports of hippocampal MRS presented quantification results only as ratios to total creatine (tCr) (17,18). Furthermore, scan-rescan reproducibility (19,20) was shown to be lower than in other brain regions at 1.5T (19,21,22). The complicating factors for obtaining high quality MRS data from the hippocampus include the small size of the structure, which necessitates a small voxel to minimize partial volume effects, thereby compromising the signal to noise ratio (SNR), and large susceptibility effects that lead to broad linewidths and loss of spectral resolution (15). In addition, small inconsistencies in voxel placement may lead to large variability in spectral quality between scanning sessions because of the vicinity of the structure to a region with large susceptibility changes (23).

The hippocampus has also been investigated by spectroscopic imaging (MRSI) (24,25). With the higher spatial resolution achievable with MRSI, distinct neurochemical profiles have been demonstrated recently at 7T for the anterior and posterior regions of the hippocampus (24). These studies still only reported metabolite ratios (total *N*-acetylaspartate-to-total creatine, tNAA/tCr and tNAA-to-total choline, tNAA/tCho) (24) or absolute concentrations of 3 metabolites (tNAA, *myo*-inositol, glutamate) (25). Therefore, complementary use of single voxel MRS (SVS) and MRSI is expected to provide the most comprehensive evaluation of hippocampal neurochemistry, with SVS providing extended neurochemical profiles and MRSI characterizing the spatial heterogeneity of lesions (11).

The aim of the present study was **1)** to investigate the feasibility of obtaining high quality hippocampal spectra that allow reliable quantification of a neurochemical profile using standard clinical 3T hardware and the semi-LASER sequence (26,27), which is gaining wider acceptance at high fields, and **2)** to establish inter-session reproducibility of hippocampal MRS, including reproducibility of voxel placement, spectral quality and neurochemical concentrations. We utilized a single-voxel, short-echo semi-LASER sequence because it minimizes chemical shift displacement errors (CSD) that are particularly large with vendor-provided protocols at 3T, and provides longer apparent T₂ relaxation times and attenuated J-evolution relative to conventional Hahn spin echo sequences, excellent water suppression and a gradient scheme optimized to generate artifact-free single shots (26,28). The sequence further allows retrospective correction of motion artifacts by saving each FID separately and correcting for frequency and phase shifts that result from subject motion and eliminating those shots that show evidence of substantial motion.

EXPERIMENTAL DETAILS:

Participants

Ten healthy volunteers (3 males, 7 females, mean age 37 ± 10 years) were enrolled in the study. All subjects signed an informed consent form according to the procedures approved by the Institutional Review Board at the University of Minnesota. Each subject was scanned in two

sessions performed 34 ± 30 days (mean \pm SD) apart. Data acquisition and all post-processing steps were performed by a single operator (P.B.).

Data acquisition

The study was performed at a 3T Siemens Tim Trio scanner (Siemens Medical Solutions, Erlangen, Germany) with body coil excitation and the standard 32-channel receive-array Siemens head coil. The shoulders of the subjects were supported by a 3cm-thick pad with the head being slightly hyperextended in order to get the long axis of the hippocampus aligned closer to the transversal plane as suggested previously (15). High-resolution sagittal MPRAGE images ($T_R = 2530$ ms, $T_E = 3.65$ ms, flip angle = 7° , slice thickness = 1 mm, 224 slices, field-of-view = 256×176 mm², matrix size = 256×256) were obtained. The spectroscopic volume of interest (VOI) $13 \times 26 \times 12$ mm³ (~ 4 mL) was placed in the left hippocampus. The VOI was inclined by 20 - 35° in one dimension on the sagittal images (Fig. 1), to align it with the long axis of the hippocampal body. Due to known susceptibility differences between tissues in the anterior part of the hippocampus (29), the most anterior part of hippocampus and amygdala were not included in the VOI. Left-right voxel position was adjusted on transversal images aligning the lateral border of the VOI and lateral part of the hippocampus while minimizing the inclusion of the ventricular temporal horn. The VOI placement in the second scanning session was independent of the first session and was based on these anatomical landmarks rather than the images from the first session.

The first and second order shims were adjusted with the echo-planar version of FASTMAP (30) (number of echoes = 8, bar thickness = 5 mm, bar FOV = 300 mm, excite pulse duration = 512 ms, refocusing pulse duration = 768 ms). MRS data were acquired with the optimized semi-LASER localization sequence (26,28) ($T_E = 28$ ms, $T_R = 5$ s) with integrated water suppression (VAPOR) and outer-volume-suppression (OVS) modules (31). The thickness of the OVS bands were set to 80 mm in all axes (x, y, z) and their distance from the VOI was 7 mm. B_1 levels required for the slice selective, asymmetric 90° pulse were adjusted for each VOI by monitoring the signal intensity whilst increasing the RF power and choosing the RF power setting that produced the maximum signal. The B_1 for the adiabatic full passage and OVS pulses was automatically set relative to the 90° pulse. In addition, the power for the VAPOR pulses was calibrated for optimum water suppression in each VOI. The signals from the 32 receive channels

were combined after adjustment for the phase shifts and scaling of the signal amplitudes based on the coil sensitivities (32). The metabolite spectra were acquired in ~5 min (64 transients). Single shot data were saved separately for further post-processing. Two unsuppressed water signals were acquired to correct for residual eddy currents and as an internal reference for metabolite quantification (28).

Segmentation

In order to assess the consistency in the voxel positioning between sessions, the within-VOI brain tissue was classified with segmentation of the MPRAGE images. Probabilistic maps of the gray matter (GM), white matter (WM) and cerebrospinal fluid (CSF) were derived by segmenting the 3D MPRAGE image using SPM8 software package (22). An in-house written MATLAB script was used to determine within-VOI fraction of GM, WM and CSF by using the iterative method of threshold selection (33) and mask of the VOI obtained for each session. Moreover, in order to assess the fraction of the hippocampus that was included in the VOI, the volume of the whole hippocampus was calculated by the standard segmentation algorithm implemented in Freesurfer software package (34).

MRS – postprocessing and quantification

Prior to summation, the single scans of metabolite spectra were corrected for small frequency and phase fluctuations and residual eddy currents were removed (35). No water removal or baseline correction was applied. All post-processing steps were performed automatically with in-house developed software. Summed spectra from each session were analyzed with LCModel (version 6.3-0G) (36). The basis set for LCModel contained 18 brain metabolites simulated with the density matrix approach (37): Ascorbate (Asc), aspartate (Asp), creatine (Cr), phosphocreatine (PCr), γ -aminobutyric acid (GABA), glucose (Glc), glutathione (GSH), glutamine (Gln), glutamate (Glu), *myo*-inositol (*myo*-Ins), *N*-acetylaspartate (NAA), *N*-acetyl-aspartyl-glutamate (NAAG), glycerophosphocholine (GPC), phosphoethanolamine (PE), phosphocholine (PCho), lactate (Lac), *scyllo*-inositol (*scyllo*-Ins) and taurine (Tau) as well as the spectrum of the macromolecules measured from occipital cortex as described previously (28). The validity of using a general macromolecule spectrum obtained in the occipital cortex was recently demonstrated (38). Spectra were analyzed in the frequency range 0.5-4.2 ppm and the

zero- and first- order phases were fixed to zero during the analysis (for LCModel parameters see our previous work (28)).

The water scaling option in LCModel was used to quantify metabolite concentrations, utilizing the unsuppressed water spectrum as an internal reference. Since the transverse relaxation is known to differ across brain regions (39), the T_2 of the tissue water was measured in the hippocampus of three subjects by acquiring a series of unsuppressed water signals at different echo times ($T_E=28-4000$ ms, $T_R=15$ s) and fitting the integrals of the water peaks by a bi-exponential function. For the biexponential fit, T_2 of CSF was fixed at 740 ms, which was measured with the same semi-LASER sequence from a small voxel (0.125-0.360 mL) from the lateral ventricles in 4 healthy subjects ($T_E = 28-4000$ ms, $T_R = 15$ s). The T_2 relaxation of tissue water obtained in hippocampus ($T_2 = 74.1 \pm 1.1$ ms, mean \pm SD) was taken into account in LCModel fitting, assuming that the T_2 of water under Carr-Purcell conditions is $1.5\times$ longer than the measured free precession T_2 (28). The smaller effect of T_2 relaxation of metabolite signals was neglected (28). The brain water content was derived assuming 81% of water in GM, 71% in WM and 100% in CSF (40). Average GM (63.8%), WM (32.7%) and CSF (3.4%) within-VOI fraction was calculated for our group of subjects (from all 20 sessions) and the average brain water content 78% ($0.81 \times 0.64 + 0.71 \times 0.33 + 1.00 \times 0.03$) was used to correct metabolite concentrations. The CSF within-VOI fraction obtained for each session (as described above) was used to correct concentrations from each session.

Previously published reliability criteria were used for reporting neurochemical concentrations (28). Namely, metabolites were considered reliably quantified if the estimated error of the quantification i.e. Cramér-Rao Lower Bounds (CRLBs) were $< 50\%$ in at least 5 of 10 scans in both sessions (visit #1, visit #2). In addition, metabolite concentrations were reported only as a sum when the pair of metabolites correlated strongly to each other ($r < -0.7$), as in the case of Cr and PCr. They were reported both separately and as a sum when correlation coefficients were in the range $-0.5 > r > -0.7$, as in the case of Glc and Tau, as recommended in the LCModel manual (36).

In order to assess spectral quality, SNR of the metabolite spectra and linewidth (LW) of the unsuppressed water spectrum were evaluated. SNR was measured as a ratio of the NAA methyl

resonance at 2.02 ppm and root mean square of the noise on the summed spectrum from each session (64 averages). LW was measured as full-width-at-half-maximum of the water spectrum.

Statistics

CRLBs, SNR, LW and the within-VOI hippocampal volumes were compared between the two sessions with the two-tailed paired t-test. The pair-wise analysis of within-VOI fractions of the GM, WM and CSF was performed using the Wilcoxon Signed Rank test. The threshold of statistical significance was set at $p = 0.05$. Pearson's correlation coefficients were obtained to compare within-VOI CSF fraction, LW and SNR between sessions.

The between-session reproducibility of metabolite concentrations was assessed by calculating coefficients-of-variance ($CV = SD/mean$) for each subject ($n = 10$) and then averaging to obtain mean between-session CVs for each metabolite. The between-session CVs for the within-VOI fractions of GM, WM and CSF were also obtained. In order to describe variability of metabolite concentrations and voxel composition (GM, WM, CSF fraction) between subjects, between-subject CVs were calculated as $SD/mean$ of the between-session averaged values. To assess whether variability in concentrations is partly due to between-person variability in voxel composition (GM, WM fraction) or spectral quality (LW, SNR), we also fit a linear mixed model for each metabolite with those four characteristics as predictors. The linear mixed model included a random effect for person to account for the within-person correlation in measured concentrations.

RESULTS:

Brain tissue segmentation confirmed consistency in the VOI placement between sessions (see Fig. in Supplementary Materials. Pairwise comparison of the within-VOI fractions of GM, WM and CSF did not reveal significant differences in GM and WM fractions between sessions, but showed a trend in the CSF fraction ($p = 0.02$). Therefore the CSF fraction from each session was used to correct the metabolite concentrations. The between-session CVs for the within-VOI fractions of GM, WM and CSF are shown in Table 1 and demonstrate excellent test-retest reproducibility of voxel composition. Mean volume of the whole hippocampus obtained from Freesurfer was $4261 \pm 640 \text{ mm}^3$ in session #1 and $4184 \pm 582 \text{ mm}^3$ in session #2 (mean \pm SD) and the mean fraction of the hippocampal volume that was included in the VOI was $61.9 \pm 6.9\%$

and $62.0 \pm 7.5\%$ for session #1 and session #2, respectively. We did not observe a significant difference in within-VOI hippocampal volume between sessions.

High reproducibility of the spectral pattern and quality (SNR, spectral resolution, water and unwanted coherence suppression) between subjects and between the two sessions is demonstrated in Figure 2. Notably, spectral patterns appeared subject-specific (note the ratios of the major metabolite peaks in each subject in Fig. 2a). An example of the LCModel analysis of a spectrum acquired in ~5 min, demonstrating the quality of spectral fitting routinely achieved in this study, is presented in Fig. 1. The mean concentrations, CRLBs and between-session CVs of metabolites that met our abovementioned reliability criteria are presented in Fig. 3. The metabolite concentrations and CRLBs were not significantly different between-sessions and the correction for the small CSF fraction (3-4%) in the hippocampus VOI did not affect the test-retest reproducibility of neurochemical concentrations, as expected.

The spectral quality allowed quantification of tNAA, NAA, Glu+Gln (Glx), tCho, tCr, Glu and *myo*-Ins with between session CVs of 6% or less and CRLB below 10% (Fig. 3b). Glc +Tau and Asc+GSH had CRLBs < 20% and five other metabolites Asc, Glc, GSH, *scyllo*-Ins and PE were quantified with mean CRLBs < 30% (Fig. 3b). Test-retest CVs and CRLBs were comparable per metabolite. While they showed great variance *across* metabolites when expressed in percent (Fig. 3b), they were more uniform across metabolites when expressed in absolute units (Fig. 3c).

Metabolite concentrations and three factors that are known to affect metabolite levels (within-VOI CSF fraction, LW and SNR) were also compared using Pearson's correlations between sessions (Fig. 4). Fig. 4a demonstrates the reproducibility for the most reliably quantified metabolite concentrations (CRLB < 9%). LW and SNR were highly reproducible between sessions, with mean test-retest CVs of 5-6% (Table 1). Consistently, the water LW and SNR correlated significantly between session #1 and session #2 ($R = 0.76$, $p = 0.01$ for LW and $R = 0.80$, $p < 0.0006$ for SNR; Figures 4b,c). Similarly, CSF fractions per subject were highly correlated between sessions, indicating the subject specificity of these ($R = 0.98$, $p < 0.0001$, Fig 4d).

Given consistent voxel positioning between sessions and minimal day-to-day biological variation in the quantified neurochemicals in the healthy brain, the between-session CVs of metabolite concentrations represent the error of the measurement and/or quantification. The between-subject

CVs encompass both the measurement error and inter-individual differences, which can be detected only if the measurement error (between-session CVs and CRLBs) is smaller. In the current study, the between-session CVs appeared to be well below between-subject CVs for most metabolites (Fig. 5a). Similarly, the CRLBs tended to be lower than between-subject CVs (Fig. 5b), at least for the metabolites quantified with higher reliability (CRLBs < 20%, Figure 5c). Importantly, for almost all metabolites, the voxel composition (GM, WM fraction) and spectral quality (SNR, LW) characteristics were not predictive of concentration in the linear mixed models. For Glu, spectral quality was significantly negatively associated with concentration ($p=0.03$ after Bonferroni correction for testing line width for each of the 16 metabolites). Therefore, except for Glu, the variance in the voxel composition and spectral quality did not explain the variance in metabolite concentrations we observed in the healthy human hippocampus.

DISCUSSION:

This study demonstrated the feasibility of obtaining spectra of high quality from hippocampus, a region particularly challenging for MRS (15). Our study benefited from utilizing an in-house developed semi-LASER localization sequence implemented at high field (3T) in combination with FASTMAP B_0 shimming. The same methodology optimized for 3T was recently introduced in a 2-site study focusing on brain regions other than the hippocampus (28). Here we were able to quantify a neurochemical profile in the hippocampus with a reproducibility and quantification precision comparable to other brain regions (21,28).

Short TE semi-LASER localization provides a similar spectral pattern to that achieved with ultra-short echo STEAM, because the apparent T_2 and J evolution is reduced by the Carl-Purcell train of adiabatic pulses (41). In addition, semi-LASER provides almost two-fold increase of the SNR relative to STEAM (26). Broadband adiabatic pulses improve the slice selection profile and substantially reduce the CSD relative to the standard full signal intensity non-adiabatic localization approach (PRESS) at 3T. For example, with the vendor-provided PRESS sequence the CSD is 12-13%/ppm for the slices selected by the 180° pulses on the Tim Trio system we utilized, whereas it is 2%/ppm for the adiabatic 180° pulses in semi-LASER. Finally, the precise localization together with robust OVS and VAPOR techniques allow acquiring of spectra free of

unwanted coherences such as the out of phase signals of lipids. Note that both the semi-LASER sequence we have used in this study (26) and the FASTMAP shimming tool are now available as a work-in-progress (WIP) package on the Siemens platform.

The iterative FASTMAP protocol we used to adjust 1st and 2nd order shims led to excellent LW (below 9 Hz for water on average). The hippocampus is located close to the skull base and nasal sinuses, which have magnetic properties different from the brain causing distortions in B_0 . Since broad LWs decrease spectral dispersion and can compromise quantification (19), optimal adjustment of B_0 field within the spectroscopy voxel was crucial in the hippocampal region. Interestingly, the LW achieved in our study ranged from 7-11.4 Hz among the 10 subjects and correlated significantly between sessions (Fig 4b). We have demonstrated a similar correlation between LW achieved at 4T and 7T in individual subjects (42). These findings indicate that between-subject variance (Table 1) results to a large extent from inter-individual differences in the (microscopic) magnetic susceptibility of the brain tissue within the VOI. In addition, the location of the VOI within the brain, such as its distance from the skull base may affect the achieved LW. The variation of LW affected the variation of SNR (Fig. 4b,c, Table 1), which is further influenced by other subject-specific factors such as coil loading. The high reproducibility of LW and SNR within subjects likely contributed to the high between-session reproducibility of metabolite concentrations.

The high SNR achieved in our study thanks to the full intensity localization sequence and the high-field system, allowed us to use a small VOI (~4mL). The relatively small voxel reduced partial volume effects and avoided the structures surrounding the hippocampus (parahippocampal gyrus, thalamus), as well as areas with increasing susceptibility effects (amygdala) (15). We were able to include ~64 % of the hippocampal GM within our VOI, consistent with other studies (40) and we covered ~62% of the total hippocampal volume. We further found that the correction for the small CSF fraction in the VOI (3-4 %) had a negligible effect on metabolite levels and their reproducibility in the healthy cohort. Nonetheless, this correction will likely be critical when clinical populations with hippocampal atrophy are studied (40). Similarly, the correction of metabolite concentrations for the effect of T_2 relaxation might be valuable when healthy volunteers are compared with clinical populations, since the T_2 of brain water and metabolites may differ between groups (43).

The CRLBs, a measure of quantification precision provided by LCModel, observed in our study were improved and allowed reliable quantification of more metabolites than prior studies (10,15,20). We were able to quantify 6 metabolites with CRLBs below 9% (Table 2) and another 4-5 metabolites with CRLBs below 20%. Therefore, the current study provides the most detailed in vivo characterization of the human hippocampal neurochemistry obtained with widely available clinical hardware. The neurochemical profile was consistent with other studies, e.g. we observed higher *myo*-Ins and lower NAA than in neocortical tissues due to a higher glial and lower neuronal density (19,20). The CRLB obtained from the hippocampus with our approach were comparable to CRLB reported from other brain regions (28).

Notably, the SNR and spectral resolution achieved in our study was sufficient to separately quantify Glu and Gln resonances. Even though these metabolites correlated moderately ($r \sim -0.5$), they could be quantified reproducibly between sessions (Fig. 3). Hippocampal Glu is a metabolite of particular clinical interest as demonstrated in studies seeking surrogate markers for diagnostics (4,40) or therapy monitoring in Alzheimer's disease (10,44) and schizophrenia (14).

The between-session CVs reported in prior test-retest studies (19,20,22,45) of the hippocampus were substantially higher than our findings. We observed 7 metabolites with between-session CVs $\leq 6\%$ (Table 2), whereas CVs previously reported at 1.5T were in the range 7-20% (for tNAA, tCho, *myo*-Ins, tCr, Glx) (19)(20). In a study conducted at 3T (45), between-session CVs were 5% for tNAA, above 7% for tCr, tCho, *myo*-Ins and 22% for Glx when using LASER with $T_E = 65$ ms. In another study the average between-session CV for tNAA, tCho and tCr was 13.9%, despite using higher field (4 T) (22), demonstrating the importance of utilizing carefully optimized methodology in addition to high field strength for optimal spectral quality.

While between-subject CVs determine the ability of the method to reveal group differences in cross-sectional studies, low test-retest CVs are critical for clinical utility and planning of longitudinal studies as they will allow detection of small changes with disease progression or in response to treatment in individuals. Interestingly, between-session CVs improved relative to prior studies, but the between-subject CVs (Table 2) remained comparable to other studies from hippocampus (19) and other brain regions (28). Therefore the improvements afforded with the novel MRS methodology primarily will benefit longitudinal studies, such as clinical trials, when pre- vs. post-treatment differences are evaluated. Our data also indicate that the relatively high

between-subject variance is due to real inter-individual differences in metabolite concentrations, except in the case of Glu, rather than due to variance in the voxel composition and spectral quality (SNR, LW). Therefore the lower between-session CVs than between-subject CVs demonstrate an ability to measure real inter-individual differences in metabolite concentrations in the healthy brain, as well as the potential to reveal subtle changes caused by pathology in individuals. Consistently, the CRLBs of the metabolites quantified with higher quantification precision (CRLB < 25 %, Figure 5c), were also lower than between-subject CVs, as in our prior studies (28,42).

Finally, this study demonstrated that an experienced operator can select the VOI highly reproducibly between sessions and subjects (Supplementary Fig.). Note however that potential operator dependence of the VOI selection is a limitation of the current protocol. While acquisition of data by a single operator is common in the research setting, methods to automatically prescribe VOI, especially in regions with large susceptibility changes such as the hippocampus (23), are critical for wider utility of the method in the clinical setting with multiple operators.

CONCLUSION:

High spectral quality can be obtained reproducibly from a ~4mL hippocampal voxel with minimal partial voluming using standard 3T hardware, an in-house implemented short echo, single voxel pulse sequence and 5 min data averaging. These spectra allow the reliable quantification of a neurochemical profile from this challenging VOI. Namely, tNAA, NAA, tCho, tCr, *myo*-Ins and Glu can be quantified with high scan-rescan reproducibility (CV ≤ 6%) and quantification precision (CRLB < 9%). Seven other metabolites, including glucose, glutathione and ascorbate, are quantified with CRLB < 30%. Finally, for most metabolites, the method has sufficient sensitivity to detect inter-individual differences in the healthy brain. Thus this novel methodology can be utilized in a broad range of clinical research applications focused on hippocampal neurochemistry altered by diseases such as Alzheimer's disease, epilepsy, schizophrenia and depression, and particularly will benefit studies of the neurochemical response evoked by therapies.

Acknowledgements:

This work was supported by the NIH grant R01 NS035192 (E.R.S., G.Ö.), and by the project “CEITEC - Central European Institute of Technology” (CZ.1.05/1.1.00/02.0068) subsidized from the European Regional Development Fund. A.M. was supported by Clinical and Translational Science Award 5KL2TR113. The Center for MR Research is supported by National Center for Research Resources (NCRR) biotechnology research resource grant P41 RR008079, National Institute of Biomedical Imaging and Bioengineering (NIBIB) grant P41 EB015894 and the Institutional Center Cores for Advanced Neuroimaging award P30 NS076408. The authors thank Dr. Silvia Mangia and, Dr. Ivan Tkáč for discussions about the MRS data analysis and the staff of the Center for MR Research for maintaining and supporting the MR systems and help with subject recruitment.

Bibliography:

1. Squire LR, Stark CE, Clark RE. The medial temporal lobe. *Annu Rev Neurosci* 2004;27:279-306.
2. Jacobson L, Sapolsky R. The role of the hippocampus in feedback regulation of the hypothalamic-pituitary-adrenocortical axis. *Endocr Rev* 1991;12(2):118-134.
3. Dixon RM, Bradley KM, Budge MM, Styles P, Smith AD. Longitudinal quantitative proton magnetic resonance spectroscopy of the hippocampus in Alzheimer's disease. *Brain* 2002;125(Pt 10):2332-2341.
4. Riederer F, Bittsanský M, Schmidt C, Mlynárik V, Baumgartner C, Moser E, Serles W. 1H magnetic resonance spectroscopy at 3 T in cryptogenic and mesial temporal lobe epilepsy. *NMR Biomed* 2006;19(5):544-553.
5. Heckers S. Neuroimaging studies of the hippocampus in schizophrenia. *Hippocampus* 2001;11(5):520-528.
6. Warner-Schmidt JL, Duman RS. Hippocampal neurogenesis: opposing effects of stress and antidepressant treatment. *Hippocampus* 2006;16(3):239-249.
7. Karl A, Schaefer M, Malta LS, Dorfel D, Rohleder N, Werner A. A meta-analysis of structural brain abnormalities in PTSD. *Neurosci Biobehav Rev* 2006;30(7):1004-1031.
8. den Heijer T, Vermeer SE, van Dijk EJ, Prins ND, Koudstaal PJ, Hofman A, Breteler MMB. Type 2 diabetes and atrophy of medial temporal lobe structures on brain MRI. *Diabetologia* 2003;46(12):1604-1610.
9. Erickson K, Voss M, Prakash R, Basak C, Szabo A, Chaddock L, Kim J, Heo S, Alves H, White S, Wojcicki T, Mailey E, Vieira V, Martin S, Pence B, Woods J, McAuley E, Kramer A. Exercise training increases size of hippocampus and improves memory. *PNAS* 2011;108(7):3017-3022.
10. Bartha R, Smith M, Rupsingh R, Rylett J, Wells JL, Borrie MJ. High field (1)H MRS of the hippocampus after donepezil treatment in Alzheimer disease. *Prog Neuropsychopharmacol Biol Psychiatry* 2008;32(3):786-793.
11. Oz G, Alger J, Barker P, Bartha R, Bizzi A, Boesch C, Bolan P, Brindle K, Cudalbu C, Dincer A, Dydak U, Emir U, Frahm J, Gonzalez R, Gruber S, Gruetter R, Gupta R, Heerschap A, Henning A, Hetherington H, Howe F, Huppi P, Hurd R, Grp MC. Clinical Proton MR Spectroscopy in Central Nervous System Disorders. *Radiology* 2014;270(3):658-679.
12. Willmann O, Wennberg R, May T, Woermann FG, Pohlmann-Eden B. The role of 1H magnetic resonance spectroscopy in pre-operative evaluation for epilepsy surgery. A meta-analysis. *Epilepsy Res* 2006;71(2-3):149-158.

13. Brazdil M, Mikl M, Chlebus P, Pazourkova M, Novak Z, Chrastina J, Prasek J, Bolcak K, Fojtikova D, Horky J, Tomcik J, Lzicarova E, Rektor I. Combining advanced neuroimaging techniques in presurgical workup of non-lesional intractable epilepsy. *Epileptic Disord* 2006;8(3):190-194.
14. Marsman A, van den Heuvel MP, Klomp DW, Kahn RS, Luijten PR, Hulshoff Pol HE. Glutamate in schizophrenia: a focused review and meta-analysis of ¹H-MRS studies. *Schizophr Bull* 2013;39(1):120-129.
15. Choi CG, Frahm J. Localized proton MRS of the human hippocampus: metabolite concentrations and relaxation times. *Magn Reson Med* 1999;41(1):204-207.
16. Reyngoudt H, Claeys T, Vlerick L, Verleden S, Acou M, Deblaere K, De Deene Y, Audenaert K, Goethals I, Achten E. Age-related differences in metabolites in the posterior cingulate cortex and hippocampus of normal ageing brain: a ¹H-MRS study. *Eur J Radiol* 2012;81(3):e223-231.
17. Brazdil M, Marecek R, Fojtikova D, Mikl M, Kuba R, Krupa P, Rektor I. Correlation study of optimized voxel-based morphometry and (¹H) MRS in patients with mesial temporal lobe epilepsy and hippocampal sclerosis. *Hum Brain Mapp* 2009;30(4):1226-1235.
18. Kraguljac NV, White DM, Reid MA, Lahti AC. Increased hippocampal glutamate and volumetric deficits in unmedicated patients with schizophrenia. *JAMA Psychiatry* 2013;70(12):1294-1302.
19. Geurts JJ, Barkhof F, Castelijns JA, Uitdehaag BM, Polman CH, Pouwels PJ. Quantitative ¹H-MRS of healthy human cortex, hippocampus, and thalamus: metabolite concentrations, quantification precision, and reproducibility. *J Magn Reson Imaging* 2004;20(3):366-371.
20. Hammen T, Stadlbauer A, Tomandl B, Ganslandt O, Pauli E, Huk W, Neundorfer B, Stefan H. Short TE single-voxel ¹H-MR spectroscopy of hippocampal structures in healthy adults at 1.5 Tesla--how reproducible are the results? *NMR Biomed* 2005;18(3):195-201.
21. Terpstra M, Emir UE, Eberly LE, Öz G. Test-retest repeatability of human neurochemical profiles measured at 3 versus 7 T [abstr]. In: *Proceedings of the 20th Meeting of the International Society for Magnetic Resonance in Medicine*. Berkeley, USA, 2012; 1739.
22. Venkatraman TN, Hamer RM, Perkins DO, Song AW, Lieberman JA, Steen RG. Single-voxel ¹H PRESS at 4.0 T: precision and variability of measurements in anterior cingulate and hippocampus. *NMR Biomed* 2006;19(4):484-491.
23. van der Kouwe AJ, Balasubramanian M, Busa EA, Fishl B. Automatic prospective spectroscopy VOI placement based on brain segmentation [abstr.]. In: *Proceedings of the 15th Meeting of the International Society for Magnetic Resonance Imaging*, Berlin, Germany, 2007; 773.
24. Hetherington HP, Hamid H, Kulas J, Ling G, Bandak F, de Lanerolle NC, Pan JW. MRSI of the medial temporal lobe at 7 T in explosive blast mild traumatic brain injury. *Magn Reson Med* 2014;71(4):1358-1367.
25. Prinsen H, Heerschap A, Bleijenberg G, Zwarts MJ, Leer JW, van Asten JJ, van der Graaf M, Rijpkema M, van Laarhoven HW. Magnetic resonance spectroscopic imaging and volumetric measurements of the brain in patients with postcancer fatigue: a randomized controlled trial. *PLoS One* 2013;8(9):e74638.
26. Oz G, Tkac I. Short-Echo, Single-Shot, Full-Intensity Proton Magnetic Resonance Spectroscopy for Neurochemical Profiling at 4 T: Validation in the Cerebellum and Brainstem. *Magn Reson Med* 2011;65(4):901-910.
27. Scheenen TW, Klomp DW, Wijnen JP, Heerschap A. Short echo time ¹H-MRSI of the human brain at 3T with minimal chemical shift displacement errors using adiabatic refocusing pulses. *Magn Reson Med* 2008;59(1):1-6.
28. Deelchand DK, Adanyeguh IM, Emir UE, Nguyen TM, Valabregue R, Henry PG, Mochel F, Oz G. Two-site reproducibility of cerebellar and brainstem neurochemical profiles with short-echo, single-voxel MRS at 3T. *Magn Reson Med* 2014.

29. Arslanoglu A, Bonekamp D, Barker PB, Horská A. Quantitative proton MR spectroscopic imaging of the mesial temporal lobe. *J Magn Reson Imaging* 2004;20(5):772-778.
30. Gruetter R, Tkac I. Field mapping without reference scan using asymmetric echo-planar techniques. *Magn Reson Med* 2000;43(2):319-323.
31. Tkac I, Starcuk Z, Choi I, Gruetter R. In vivo H-1 NMR spectroscopy of rat brain at 1 ms echo time. *Magnetic Resonance in Medicine* 1999;41(4):649-656.
32. Natt O, Bezkorovaynyy V, Michaelis T, Frahm J. Use of phased array coils for a determination of absolute metabolite concentrations. *Magn Reson Med* 2005;53(1):3-8.
33. Ridler TW, Calvard S. Picture Thresholding Using an Iterative Selection Method. *Ieee Transactions on Systems Man and Cybernetics* 1978;8(8):630-632.
34. Morey RA, Petty CM, Xu Y, Hayes JP, Wagner HR, Lewis DV, LaBar KS, Styner M, McCarthy G. A comparison of automated segmentation and manual tracing for quantifying hippocampal and amygdala volumes. *Neuroimage* 2009;45(3):855-866.
35. Klose U. In vivo proton spectroscopy in presence of eddy currents. *Magn Reson Med* 1990;14(1):26-30.
36. Provencher SW. Estimation of metabolite concentrations from localized in vivo proton NMR spectra. *Magn Reson Med.* 1993; 30 : 672–679
37. Deelchand DK, Henry PG, Uğurbil K, Marjańska M. Measurement of transverse relaxation times of J-coupled metabolites in the human visual cortex at 4 T. *Magn Reson Med* 2012;67(4):891-897.
38. Schaller B, Xin L, Gruetter R. Is the macromolecule signal tissue-specific in healthy human brain? A (1)H MRS study at 7 Tesla in the occipital lobe. *Magn Reson Med* 2014;72(4):934-940.
39. Marjańska M, Auerbach EJ, Valabregue R, Van de Moortele PF, Adriany G, Garwood M. Localized 1H NMR spectroscopy in different regions of human brain in vivo at 7 T: T2 relaxation times and concentrations of cerebral metabolites. *NMR Biomed* 2012;25(2):332-339.
40. Rupasingh R, Borrie M, Smith M, Wells JL, Bartha R. Reduced hippocampal glutamate in Alzheimer disease. *Neurobiology of aging* 2011;32(5):802-810.
41. Bartha R, Michaeli S, Merkle H, Adriany G, Andersen P, Chen W, Ugurbil K, Garwood M. In vivo 1H2O T2+ measurement in the human occipital lobe at 4T and 7T by Carr-Purcell MRI: detection of microscopic susceptibility contrast. *Magn Reson Med* 2002;47(4):742-750.
42. Tkac I, Oz G, Adriany G, Ugurbil K, Gruetter R. In vivo 1H NMR spectroscopy of the human brain at high magnetic fields: Metabolite quantification at 4T vs. 7T. *Magn Reson Med* 2009;62(4):868-879
43. Marjańska M, Emir UE, Deelchand DK, Terpstra M. Faster metabolite (1)H transverse relaxation in the elder human brain. *PLoS One* 2013;8(10):e77572.
44. Penner J, Rupasingh R, Smith M, Wells JL, Borrie MJ, Bartha R. Increased glutamate in the hippocampus after galantamine treatment for Alzheimer disease. *Prog Neuropsychopharmacol Biol Psychiatry* 2010;34(1):104-110.
45. Allaili N, Marjanska M, Auerrbach EJ, Bardinet E, Fossati P, Valabregue R, Lehericy S. Single voxel 1H spectroscopy in the human hippocampus at 3T using LASER: A reproducibility study [abstr.] In: *Proceedings of the 18th Meeting of the International Society for Magnetic Resonance in Medicine*, 2010, Stockholm, Sweden; 939

Figure captions:

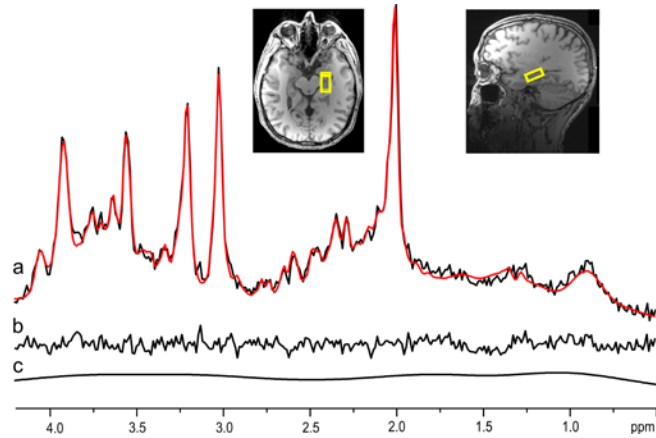
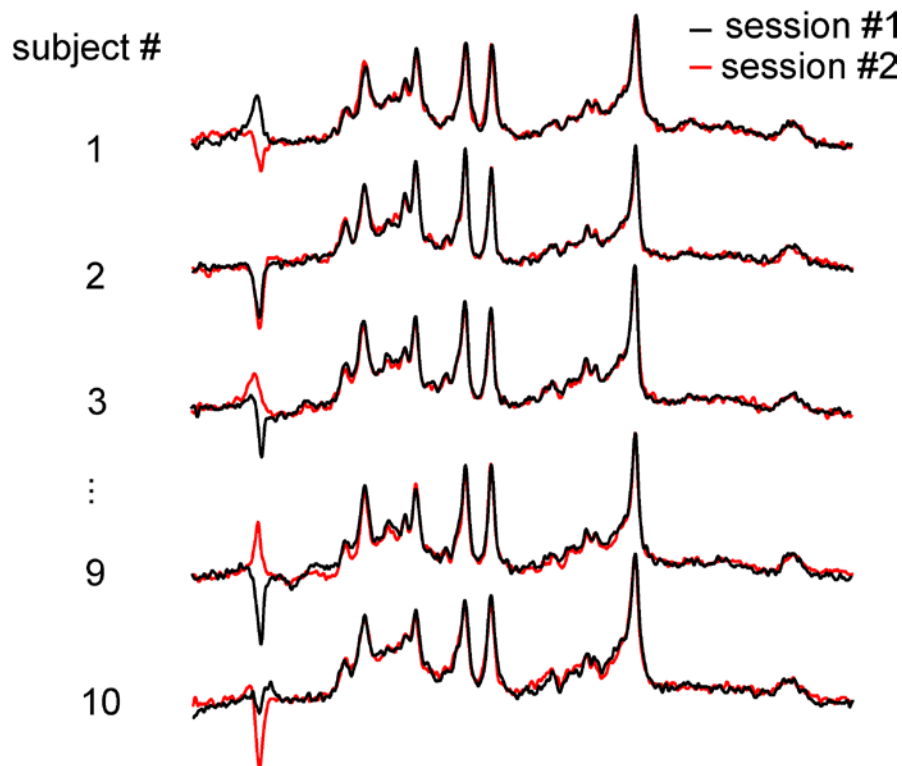


Figure 1. Fitting of a sample spectrum with LCModel. Spectrum acquired in 5.2 min from the left hippocampus (VOI 13 x 12 x 26 mm³) with the LCModel fit overlaid in red (a). Residual (b) and baseline spline function (c) resulting from LCModel analysis are presented. No apodization filter was applied on the displayed data. Spectra acquired with semi-LASER (TR = 5 s, TE = 28 ms, 64 transients). VOI position is shown on sagittal and axial MPRAGE images.

a between-session reproducibility



b between-subject reproducibility
(n = 10)

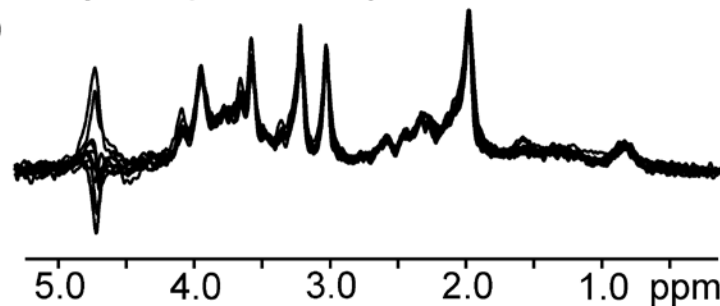


Figure 2. Between-session and between-subject reproducibility of the hippocampal spectra. (a) Spectra acquired in 5 selected healthy subjects in two consequent sessions from the hippocampus are overlaid to demonstrate between-session reproducibility of the MRS data. (b) In order to demonstrate between-subject reproducibility, the spectra from the two sessions are averaged for each subject and overlaid (n=10). NAA-methyl resonance at 2 ppm is used to scale the spectra. Gaussian apodization function ($\sigma = 0.13$ s) was used for display purposes.

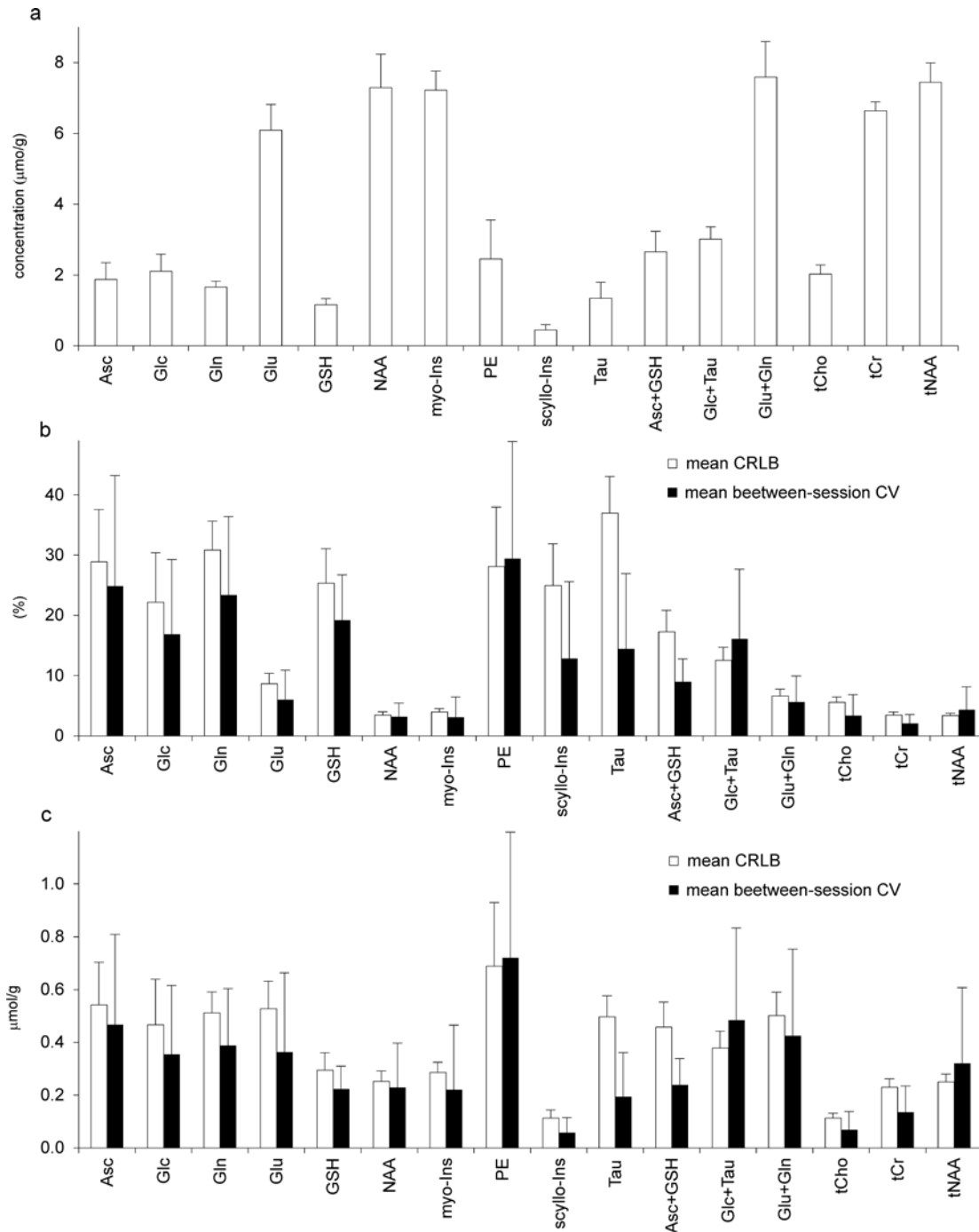


Figure 3. Group analysis of LCModel quantification. Concentrations were averaged between the two sessions for each subject and mean values calculated across 10 subjects. Concentrations corrected for CSF and tissue water T_2 relaxation are shown (a). The corresponding mean CRLBs and mean between-session coefficients of variance (CVs, SD/mean) of metabolite concentrations are shown in percent (b) and in absolute units (c). Error bars represent SDs.

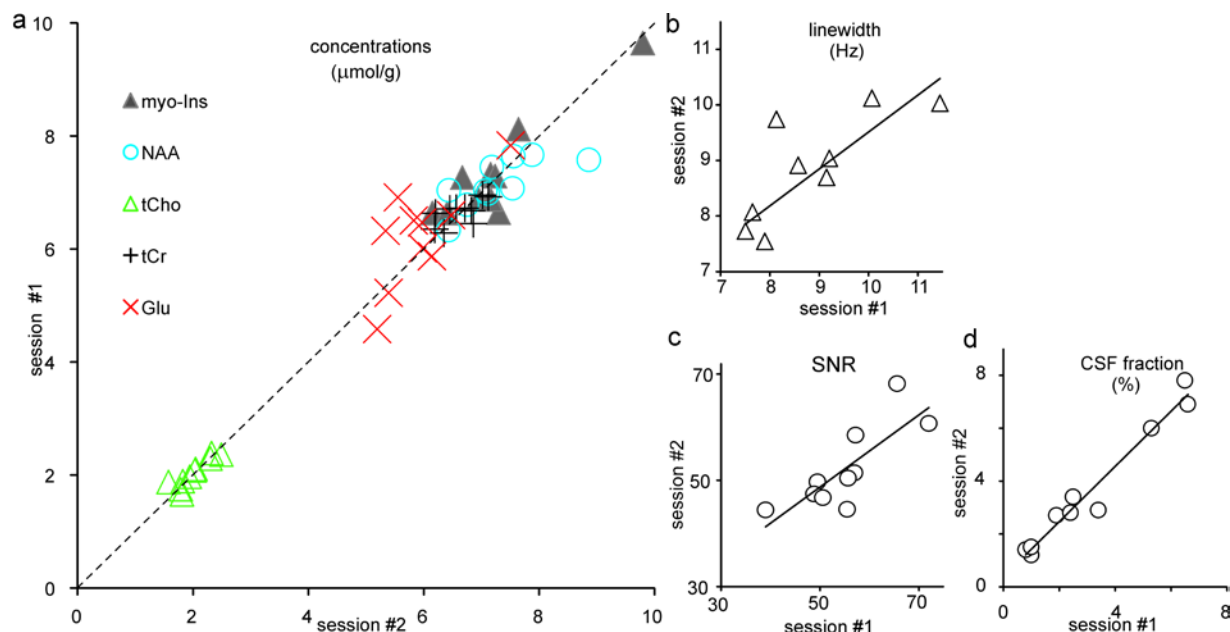


Figure 4. Reproducibility of metabolite concentrations, linewidths and SNR between sessions. Only metabolites with CRLBs < 9% are presented and concentrations of selected metabolites are distributed along identity line (a). Correlation plots demonstrate the subject-specific nature of linewidths (measured on the unsuppressed water spectra) (b), SNR (c) and within-VOI CSF fraction (d).

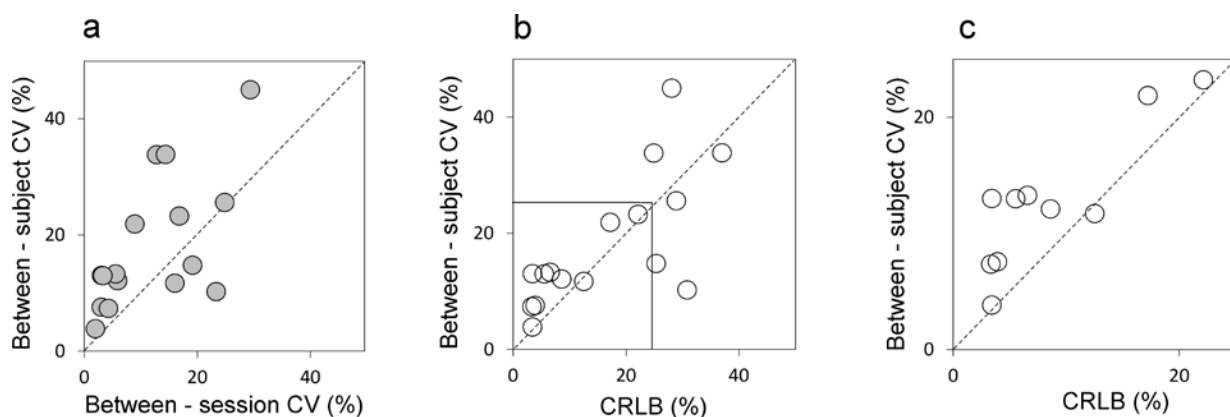


Figure 5. Comparison of between-subject and between-session variance of MRS data. Comparison of mean between-session coefficients of variation (CVs) and mean between-subject CVs (calculated from concentrations averaged between sessions per subject) (a). Comparison of mean CRLBs and mean between-subject CVs (both calculated from between-session averages) (b). (c) is a zoomed version of (b) and shows only the metabolites measured with CRLBs < 25%. Each data point represents a metabolite.

Table 1. Reproducibility of the voxel composition (white matter – WM, gray matter - GM , and cerebrospinal fluid – CSF fraction), linewidth (LW) and signal-to-noise ratio (SNR). Means are calculated from between-session averages obtained for each subject. Between-session CVs averaged across subjects are shown.

	Mean \pm SD	Mean between – session CV
WM (%)	32.7 \pm 4.6	7.5
GM (%)	63.8 \pm 4.7	3.5
CSF (%)	3.4 \pm 2.3	17.2
LW (Hz)	8.7 \pm 1.1	4.8
SNR	53.6 \pm 8.1	6.3

Table 2. Metabolites quantified with high reproducibility and quantification precision. CRLBs, between-session CVs and between-subject CVs of the metabolites that were quantified with CRLB < 9 % and between-session CVs \leq 6% are presented.

	CRLB (%)	Between-session CV (%)	Between-subject CV (%)
Glu	8.7	6.0	12.1
Glx	6.6	5.6	13.3
<i>myo</i> -Ins	3.5	3.1	13.0
tCho	5.6	3.3	13.0
tCr	3.5	2.0	3.8
NAA	4.0	3.0	7.5
tNAA	3.4	4.3	7.3

Supplementary Material:

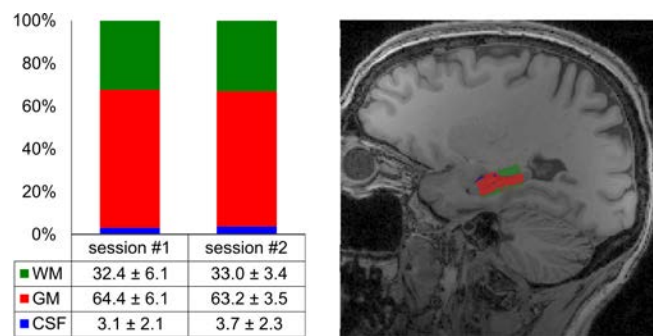


Figure. Reproducibility of voxel placement. Fractions (in %) of white matter (WM), gray matter (GM) and cerebrospinal fluid (CSF) within the spectroscopic VOI. Consistent results between two consequent sessions demonstrate reproducible VOI placement. Data are mean \pm SD.